JMEPEG (2012) 21:1687–1695
DOI: 10.1007/s11665-011-0067-1

1059-9495/$19.00

Fatigue Life of Superalloy Haynes 188 in Hydrogen

T.P. Gabb, H. Webster, G. Ribeiro, T. Gorman, and J. Gayda

(Submitted July 18, 2011)

The effects of hydrogen and surface finish on the mean low cycle fatigue life of Haynes 188 were studied. Specimens were prepared and fatigue tested with gage sections having low stress ground (LSG) and electro-discharge machined (EDM) surfaces. Fatigue tests were performed at temperatures of 25 to 650 °C with varied strain conditions, in hydrogen and helium environments. Fatigue life decreased with increasing strain range, strain ratio, temperature, and with hydrogen atmosphere. A Smith-Watson-Topper stress parameter could be used to account for variations in strain range and strain ratio, and most strongly influenced life. Hydrogen reduced fatigue life by about 5× (80%) at 25 °C, but was much less harmful at 650 °C. Standard EDM finish did not consistently reduce mean fatigue life from that of LSG finish specimens. Additional tests indicated fatigue life in hydrogen was maintained for varied EDM conditions, provided specimen roughness and maximum recast layer thickness were not excessive.

Keywords aerospace, environment, superalloys

1. Introduction

Hypersonic engine combustor and nozzle components will encounter severe conditions that could challenge the material's low cycle fatigue durability (Ref 1, 2). Some components may require fuel cooling, with internal cooling passages only millimeters in diameter for flow of liquid hydrogen. NASA is studying cooling passages that could be electro-discharge machined (EDM), with an EDM surface retained for the application. This would result in surfaces of thin panels, less than 1 cm in thickness, being exposed to liquid hydrogen, high pressure gaseous hydrogen, or hydrogen combustion environments. Transient wall temperatures quickly rise from cryogenic to near 650 °C across some sections in these applications. Such conditions produce high thermal gradients and strains across the sections, as well as the potential for hydrogen embrittlement.

Haynes 188 is a cobalt-based superalloy having a combination of high workability, ductility, and fatigue resistance at the high temperatures needed for combustor applications (Ref 3). Haynes 188 has been demonstrated to have relatively good resistance to hydrogen embrittlement in limited previous work (Ref 4). Tensile, rupture, and fatigue testing of Haynes 188 indicated that these mechanical properties were not significantly degraded in high pressure hydrogen. However, a wider range of test and surface conditions is required to screen for hydrogen fueled hypersonic component applications.

T.P. Gabb and **J. Gayda**, NASA Glenn Research Center, 21000 Brookpark Rd., Cleveland, OH 44135; **H. Webster** and **G. Ribeiro**, ATK Missile Products Group, 300 Village Square Crossing, Suite 201, Palm Beach Gardens, FL 33410; and **T. Gorman**, University of Dayton, 300 College Park, Dayton, OH 45469. Contact e-mail: tim.gabb@grc.nasa.gov.

The objective of this study is to determine the effects of hydrogen and EDM surface finish on the mean low cycle fatigue life of Haynes 188. Specimens were prepared and fatigue tested with gage sections having low stress ground (LSG) and EDM finishes. Fatigue tests were performed at temperatures of 25 and 650 °C with varied strain conditions, in hydrogen and helium environments. Additional exploratory tests were subsequently performed at additional conditions.

2. Material and Procedures

Haynes 188 material was obtained from Haynes International as hot-rolled plates about 17.8 mm in thickness. The composition in weight percent is given in Table 1. Preliminary tensile tests were performed at 25 and 650 °C in air on conventional LSG tensile specimens, having a nominal gage diameter of 4.1 mm and length of 20.8 mm. Fatigue specimens were machined using the configuration shown in Fig. 1. Some fatigue specimens were machined by low stress grinding. Others were electro-discharge machined in the gage section, using "standard" EDM machine settings potentially employed for small cooling holes as envisioned for hypersonic combustor sections. Surface roughness was screened using a Keyence VHX-600 digital optical microscope. Typical surfaces and roughness profiles are shown from the gage sections of fatigue specimens machined with LSG and standard EDM conditions in Fig. 2.

Fatigue testing was performed at the hydrogen fatigue testing facility located at NASA Marshall Space Flight Center. A majority of the fatigue tests were performed at 25 and 650 °C, in helium and hydrogen gas environments maintained at a pressure of 34.5 MPa. The tests were performed with strain controlled using triangular waveforms at a frequency of 0.167 Hz, which maintained a constant total strain range ($\Delta\varepsilon_t$) at minimum/maximum strain ratios (R_ε) of 0.05 and −1. Additional tests were performed at 325 °C in hydrogen at the same facility. Failure was defined as a 50% reduction in tensile stress from the stabilized level in each test. Fatigue test lives and failure initiation modes were subsequently determined and compared for all cases. Analyses of variance and regressions were performed using JMP® software.

3. Results and Discussion

3.1 Material

The typical microstructure consisted of a γ phase face-centered cubic matrix, with scattered W_6C phase simple cubic carbides, Fig. 3. The matrix had a mean grain size of about 40 μm. Etched metallographically prepared sections indicated a small, uncracked recast layer of up to 11 μm thickness formed on the EDM surfaces, Fig. 4. X-ray diffraction analyses, according to ASTM E915 and E1426, by Lambda Technologies indicated that the residual stresses near the machined surfaces varied significantly between the two surface conditions, Fig. 5. Compressive residual stress extending to −600 MPa was observed for a LSG specimen surface. However, tensile residual stress extended to +600 MPa for a typical EDM specimen surface, machined using the "standard" EDM conditions. Residual stresses approached zero for depths greater than 0.03 mm.

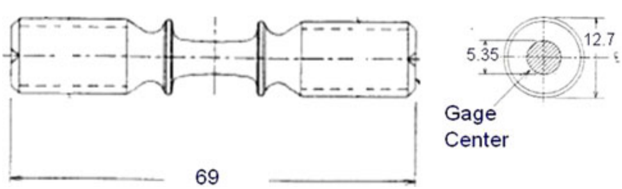

Fig. 1 Fatigue test specimen configuration, dimensions in mm

Results of duplicate tensile tests are shown in Table 2 and Fig. 6. Tensile properties did not significantly vary for specimens oriented in the plate longitudinal (*L*) and width (*W*) directions. Yield and ultimate tensile strength decreased 30 and 20%, respectively, going from 25 to 650 °C. Ductility remained very high in all tests, with over 50% reduction in area observed.

3.2 Fatigue Life Response

Fatigue lives are compared in Table 3, and shown as a function of total strain range in Fig. 7. The hydrogen environment reduced life when compared to a helium environment at 25 °C, but the effect of hydrogen was imperceptible at 650 °C. Fatigue life was also dependent on strain ratio, with increasing strain ratio reducing life. A Smith-Watson-Topper (SWT) stress parameter (σ_{SWT}) was used to account for changes in strain ratio, which influence maximum and mean stresses. This parameter is a function of total strain range ($\Delta\varepsilon_t$), maximum stress (σ_{max}), and elastic modulus (E), according to the equation (Ref 5):

$$\sigma_{SWT} = (\sigma_{max}\Delta\varepsilon_t E/2)^{0.5}$$

This fatigue parameter has worked well in past fatigue studies (Ref 6) of Haynes 188. Fatigue lives for tests at the two strain ratios converged well using σ_{SWT}, and showed that hydrogen reduced fatigue life by about 80% (5×) at 25 °C but

Table 1 Composition of Haynes 188

Element	B	C	Cr	Fe	La	Mn	Ni	Si	W	Co
Weight%	0.015(a)	0.10	22.0	3.0(a)	0.03	1.25(a)	22.0	0.35	14.0	39 (bal.)

(a) Maximum

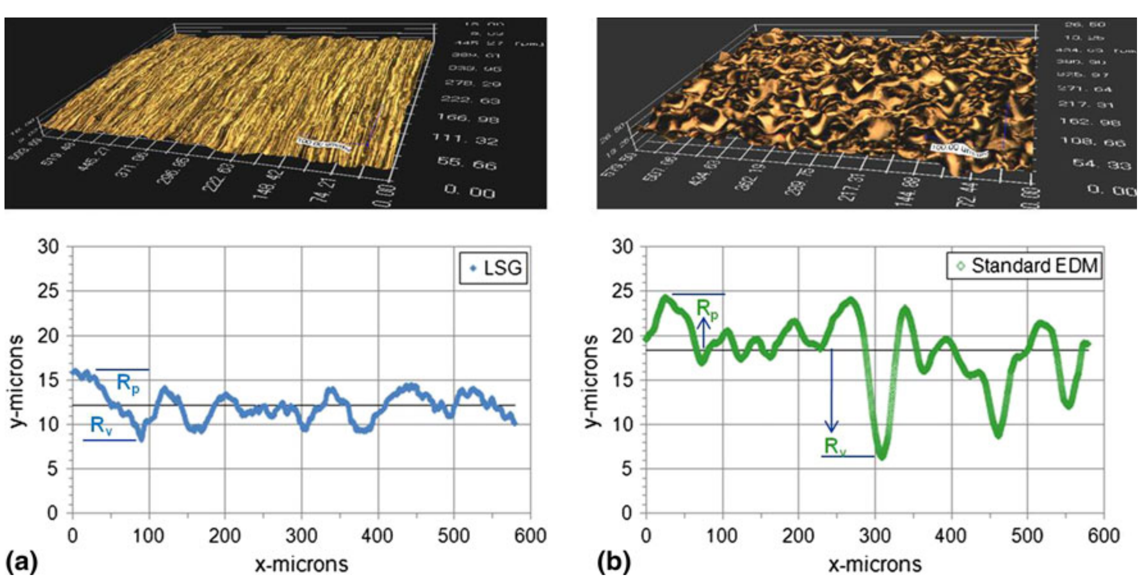

Fig. 2 Comparison of gage surfaces and roughness for fatigue specimens: (a) low stress ground and (b) standard EDM

Table 2 Tensile test results

Specimen orientation	Temperature, °C	Ultimate strength, MPa	Yield strength, MPa	Elongation, %	Red. area, %
L	RT	1014	483	50	54
W	RT	1014	490	48	52
L	650	834	299	60	56
W	650	834	316	57	53

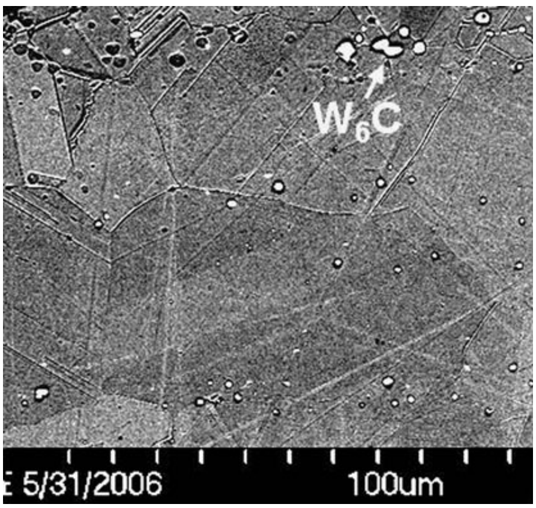

Fig. 3 Microstructure of Haynes 188 test material, made up of γ phase matrix with scattered W_6C carbides

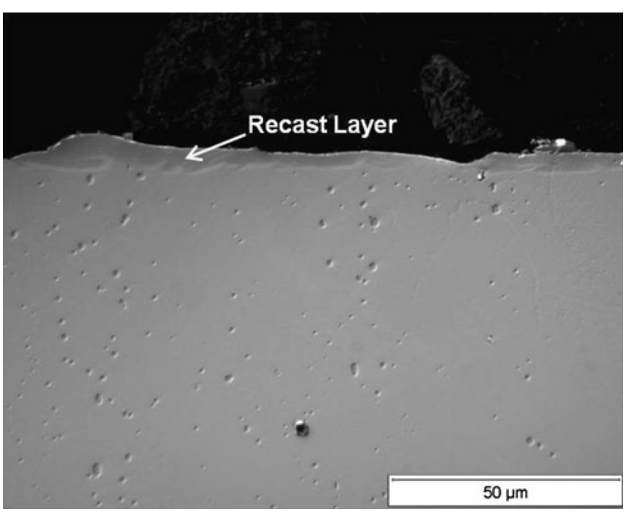

Fig. 4 "Standard" EDM recast layer on surface of fatigue specimen used in baseline tests

reduced life by less than 30% at 650 °C, Fig. 8. The EDM finish did not appear to have a consistent effect on fatigue life.

Multiple linear regression was performed to quantify these trends. The logarithm of fatigue life was regressed against environment, temperature, stress, and roughness, and all two-way interactions. A discrete, categorical variable was employed for the environment ($e = 0$ for helium, 1 for hydrogen), and continuous variables were used for temperature (T) and SWT stress (σ_{SWT}). Continuous variables of root mean square

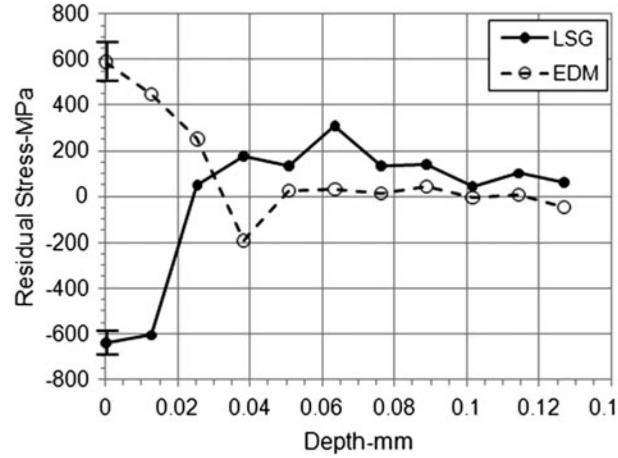

Fig. 5 Comparison of residual stresses measured on surfaces of low stress ground and EDM ("standard" conditions) fatigue specimens versus depth

roughness (R_q), peak roughness, (R_p), and valley roughness (R_v) were used to quantify LSG versus EDM surface finishes. Continuous variables (V) were transformed or "coded" (Ref 7) so that they each ranged from −1 to 1:

$$V' = (V - V_{mid})/(\Delta V/2).$$

The magnitude of regression constants in equations derived and expressed using coded variables can be used to rank the influences of all included variables. Stepwise forward and reverse sequential selections of terms were performed, with selection of all terms found significant at a probability of at least 90%. Forward and reverse stepwise selections produced an identical regression equation. The equation as expressed using coded continuous variables is:

$$\begin{aligned}\text{Log(life)} = {} & 3.7901 - 0.3678e - 0.4373T' - 0.7213\sigma'_{SWT} \\ & + 0.1843eT' - 0.1876T'\,\sigma'_{SWT}.\end{aligned}$$

This model indicated that increased σ_{SWT} most strongly reduced fatigue life, followed by increased temperature and then hydrogen environment. Two variable interaction terms had smaller, but also significant effects on fatigue life. These terms indicated life was further reduced by the combination of hydrogen with low temperature, and the combination of high temperature with high stress. Roughness did not have a significant effect on life. This model described the effects of conditions on mean fatigue life reasonably well, with a coefficient of determination, adjusted for the number of variables, of $R^2_{adj} = 0.855$, and a root mean square error in log(life) of 0.1846. Model estimates agreed well with actual lives, Fig. 9. The model expressed using continuous variables without the transformation was:

$$\begin{aligned}\text{Log(life)} = {} & 5.7777 - 0.5669e + 3.5451 \times 10^{-4}T \\ & - 2.0076 \times 10^{-3}\sigma_{SWT} + 5.8991 \times 10^{-4}eT \\ & - 2.3235 \times 10^{-6}T\sigma_{SWT}.\end{aligned}$$

Fatigue failure initiation modes are compared in Fig. 10 and 11. As previously found in fatigue crack propagation tests (Ref 8) of other superalloys, crack initiation modes were affected by high pressure hydrogen at both test temperatures. However,

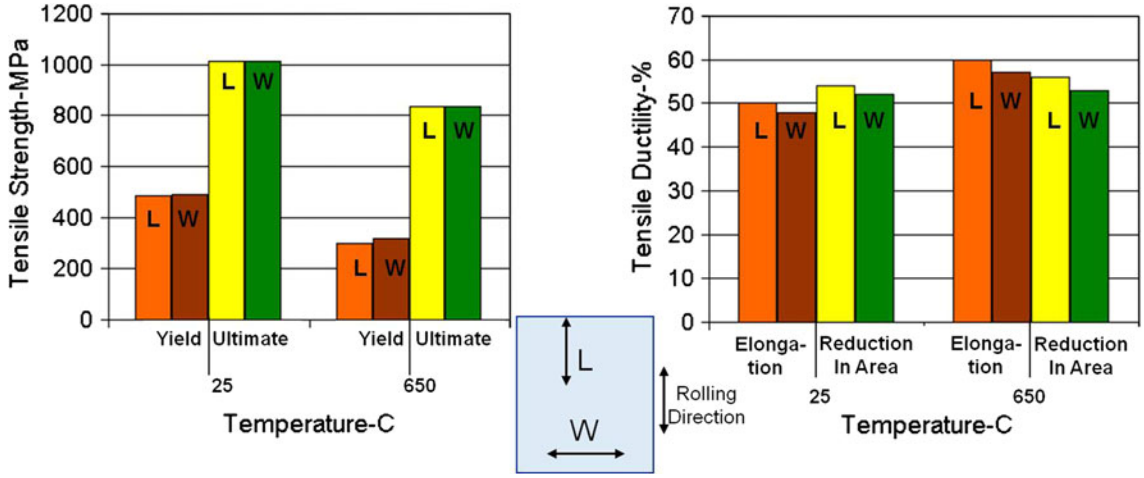

Fig. 6 Tensile properties in air, for tests at 25 and 650 °C. Specimens extracted from the rolled plate's longitudinal (*L*) and width (*W*) directions

Table 3 Fatigue test results

Condition	Environment	Temperature, °C	Elastic modulus, GPa	Total strain range, %	Strain ratio	Max. stress, MPa	Min. stress, MPa	Stress range, MPa	SWT stress, MPa	Fatigue life, cycles
Low stress ground	Helium	Room	241	0.6	−1	551	−566	1118	632	34,710
Low stress ground	Helium	Room	233	1.24	−1	710	−706	1416	1013	4,736
Low stress ground	Helium	Room	235	1.09	0.05	700	−665	1365	947	6,138
Low stress ground	Helium	Room	211	0.6086	0.05	565	−507	1072	603	57,595+
Low stress ground	Hydrogen	Room	210	0.596	−1	531	−548	1079	576	14,123+
Low stress ground	Hydrogen	Room	226	0.6	−1	555	−557	1112	613	15,045
Low stress ground	Hydrogen	Room	225	1.278	−1	629	−627	1256	952	2,091
Low stress ground	Hydrogen	Room	249	0.61	0.05	551	−503	1054	647	10,000
Low stress ground	Hydrogen	Room	251	0.98	0.05	549	−623	1172	822	1,765
Standard EDM	Hydrogen	Room	223	0.6	−1	537	−525	533	599	9,521
Standard EDM	Hydrogen	Room	222	1.227	−1	642	−647	1289	935	1,423
Standard EDM	Hydrogen	Room	249	0.59	0.05	507	−521	1028	610	6,154
Standard EDM	Hydrogen	Room	228	0.845	0.05	593	−570	1162	756	3,300
Standard EDM	Hydrogen	Room	246	0.99	0.05	685	−646	1331	913	5,971
Low stress ground	Helium	650	201	0.57	−1	507	−538	1045	539	14,136
Low stress ground	Helium	650	201	1.29	−1	658	−684	1342	923	1,133
Low stress ground	Helium	650	201	1	0.05	565	−586	1151	754	1,826
Low stress ground	Helium	650	203	1.04	0.05	593	−629	1222	791	1,453
Standard EDM	Helium	650	181	0.592	−1	460	−517	977	496	27,890
Standard EDM	Helium	650	190	1.23	−1	612	−643	1256	845	988
Standard EDM	Helium	650	191	0.606	0.05	481	−531	1011	527	9,770
Standard EDM	Helium	650	198	1.04	0.05	663	−678	1341	826	875
Low stress ground	Hydrogen	650	185	0.62	−1	467	−487	953	517	16,777
Low stress ground	Hydrogen	650	187	1.202	−1	579	−607	1186	806	1,287
Low stress ground	Hydrogen	650	197	0.59	0.05	456	−467	924	514	7,959
Low stress ground	Hydrogen	650	190	1.03	0.05	574	−584	1158	750	1,291
Standard EDM	Hydrogen	650	191	0.587	−1	443	−476	919	498	8,409
Standard EDM	Hydrogen	650	171	1.188	−1	526	−573	1099	730	1,314
Standard EDM	Hydrogen	650	197	0.59	0.05	505	−532	1037	541	12,251
Standard EDM	Hydrogen	650	179	1.01	0.05	626	−637	1263	753	1,369
Low EDM Low	Hydrogen	325	200	0.651	0.05	485	−482	967	562	27,464
Low EDM Low	Hydrogen	325	206	0.618	0.05	470	−462	931	546	27,604
Low EDM Low	Hydrogen	325	206	0.618	0.05	480	−448	928	553	29,109
Standard EDM	Hydrogen	325	205	0.603	0.05	492	−485	977	552	31,987
Standard EDM	Hydrogen	325	212	0.609	0.05	489	−471	960	562	28,278
High EDM	Hydrogen	325	209	0.605	0.05	469	−448	917	544	25,084
High EDM	Hydrogen	325	203	0.612	0.05	473	−461	934	542	19,679
High EDM	Hydrogen	325	214	0.6144	0.05	475	−443	919	559	16,844

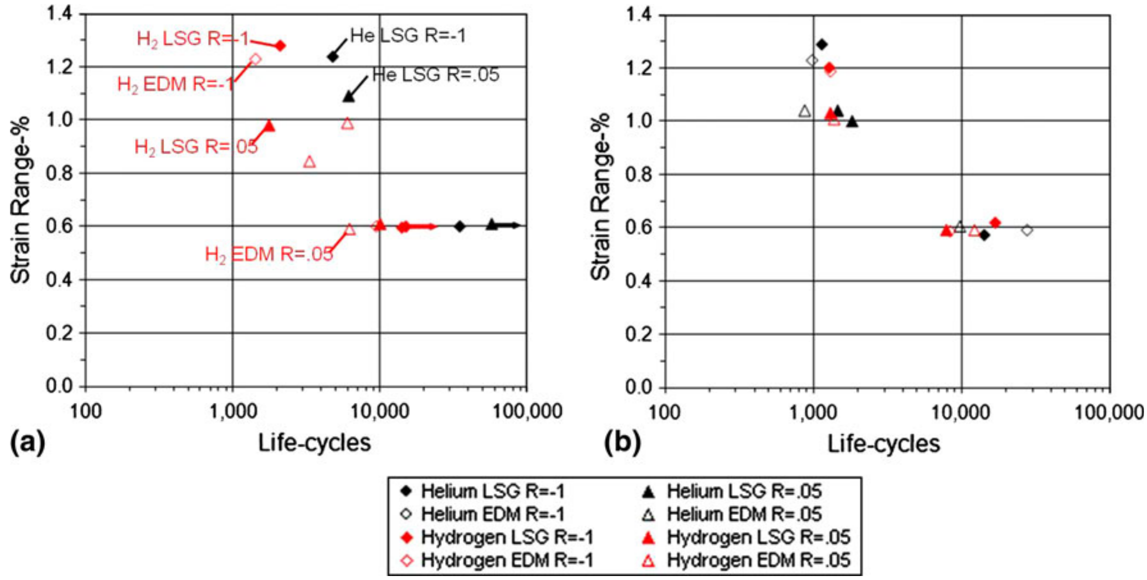

Fig. 7 Fatigue life versus strain range in helium and hydrogen, at: (a) 25 °C and (b) 650 °C

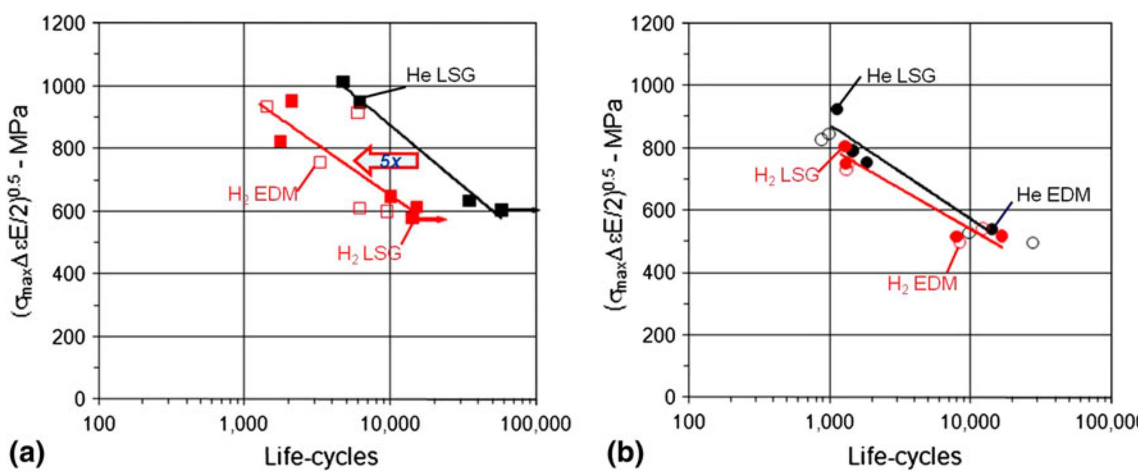

Fig. 8 Fatigue life versus Smith-Watson-Topper stress parameter (σ_{SWT}) in helium and hydrogen, at: (a) 25 °C and (b) 650 °C

fatigue failure initiation sites varied with environment, in different ways at the two test temperatures. As shown in Fig. 10, transgranular cracks initiated normal to the loading axis for tests in helium at 25 °C. However, failures initiated parallel to single crystallographic plains of large grains at the exposed surface in hydrogen. Subsequent crack growth was transgranular in both cases, but did not appear faceted or brittle. At 650 °C, hydrogen encouraged failures to initiate at grain boundaries adjacent to the specimen surface, Fig. 11. Subsequent crack growth was again transgranular, and did not appear brittle. No consistent differences were observed in failure initiation modes between LSG and EDM finish specimens. Tests at higher strain levels had more numerous fatigue crack initiation sites.

3.3 EDM Surface Variation Effects

Additional tests were performed to further investigate EDM finish. While surface roughness was not found to significantly reduce mean fatigue life, initial results suggested EDM finish could sometimes increase scatter in life, Fig. 7. This could be related to variations in surface roughness, recast layer thickness, and associated damage among EDM finish specimens. Additional specimens were prepared in which EDM condition settings were purposefully varied, which in turn varied roughness and recast layer thickness to ''low'' and ''high'' values around the ''standard'' EDM condition, roughness, and recast layer thickness previously tested, Fig. 12. Eight fatigue tests were performed in hydrogen at a fixed intermediate temperature of 325 °C, strain range of 0.6%, and strain ratio of 0.05. SWT stress was near 552 MPa in these tests, and did not vary significantly with EDM condition. Log(life) was near that at room temperature, and moderately decreased only for ''high'' EDM settings and roughness, as shown in Fig. 13. One-way ANOVA analyses indicated only the high EDM setting significantly reduced mean fatigue life, at a probability of 96%. This indicated that EDM processing could be used in the present circumstances with no significant effect on fatigue life, provided processing conditions and resulting roughness and recast layer thickness are maintained below the "high" values. Valley roughness (R_v) and maximum recast layer thickness were more significantly correlated with life than other roughness and thickness parameters, Fig. 14. However, for all these parameters, only values corresponding to the high settings gave significantly lower fatigue lives, where remnant scatter suggested the influence of additional factors.

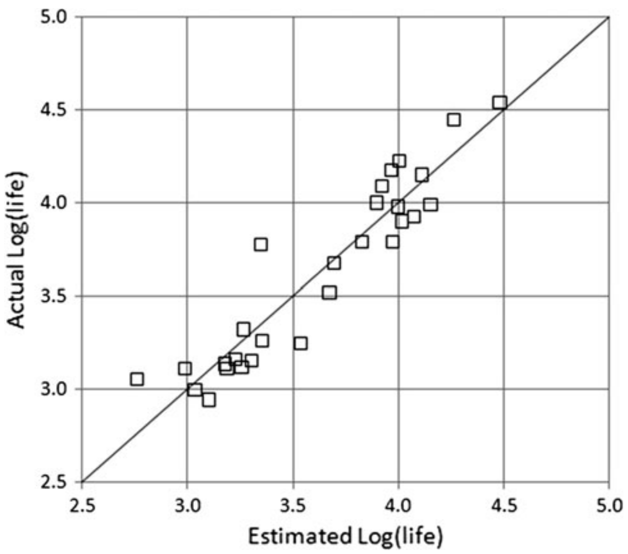

Fig. 9 Fatigue life estimated using the regression equation versus actual life, for tests in helium and hydrogen, at 25 and 650 °C

Failures initiated in these tests by transgranular cracking from the surface recast layers, as shown in Fig. 15. Subsequent fatigue crack growth remained transgranular in nature. Specimens having the high EDM settings had cracks at thicker recast layer segments and deeper roughness valleys than those for the other conditions, as shown in the metallographic sections prepared parallel to the loading condition, Fig. 16.

3.4 Overall Suitability of Haynes 188

The low cycle fatigue life capability of Haynes 188 in high pressure hydrogen appeared to be quite satisfactory for hypersonic engine applications. Life moderately decreased with increasing strain and temperature conditions, but was reduced in hydrogen by only 5× at 25 °C, and much less at 650 °C. Mean life capability was sustained even with a "standard" EDM surface preparation, potentially viable for combustor cooling holes. This could be related to the superior ductility of this material. Application of high cyclic strains would induce enhanced plastic flow and cyclic "shakedown" of maximum stresses, making the material less sensitive to EDM surface residual stresses, roughness, and recast layers. However, EDM conditions do need to be well-controlled, to not allow "high" levels of roughness and recast layer thickness that were shown to reduce fatigue life. It may be that such an EDM-fatigue response is possible for other metallic materials, in that surface preparation by carefully controlled EDM conditions

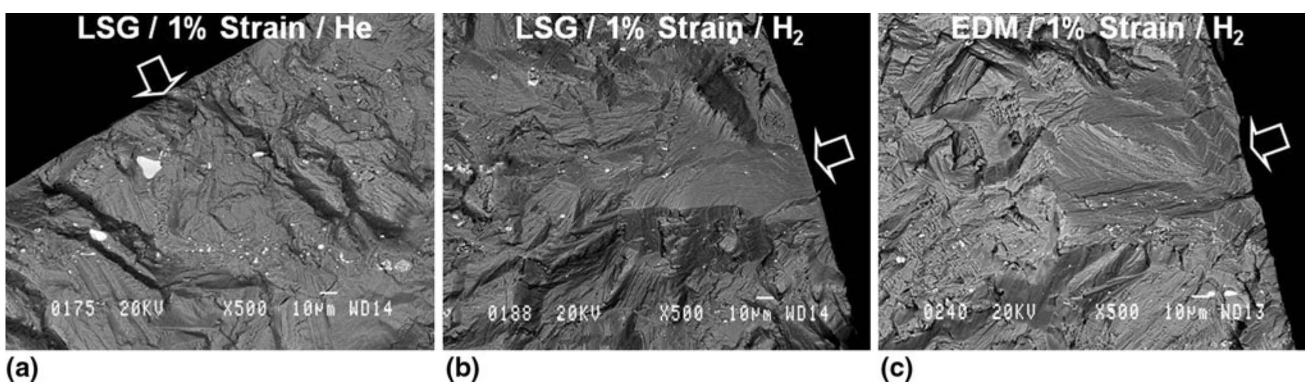

Fig. 10 Typical fatigue failure initiation sites for tests at 25 °C: (a) LSG, helium, (b) LSG, hydrogen, and (c) EDM, hydrogen

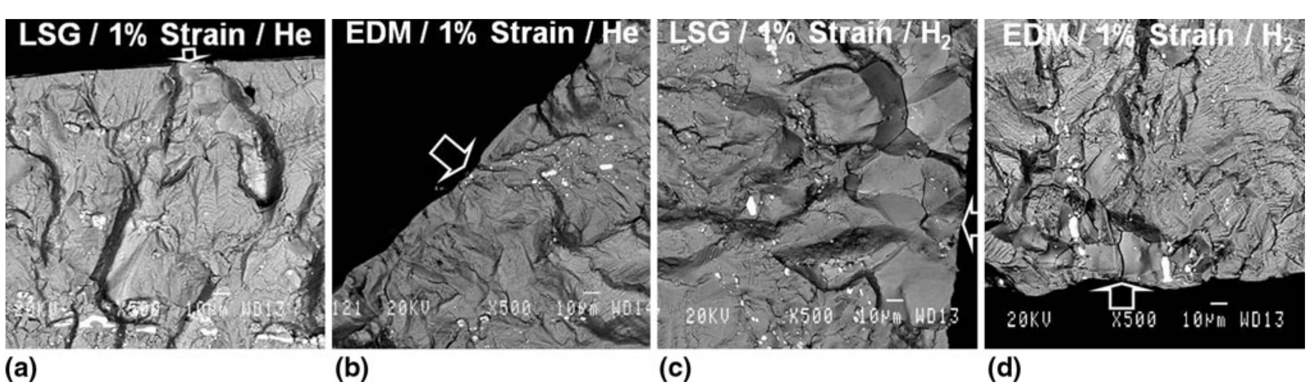

Fig. 11 Typical fatigue failure initiation sites for tests at 650 °C: (a) LSG, helium, (b) EDM, helium, (c) LSG, hydrogen, (d) EDM, hydrogen

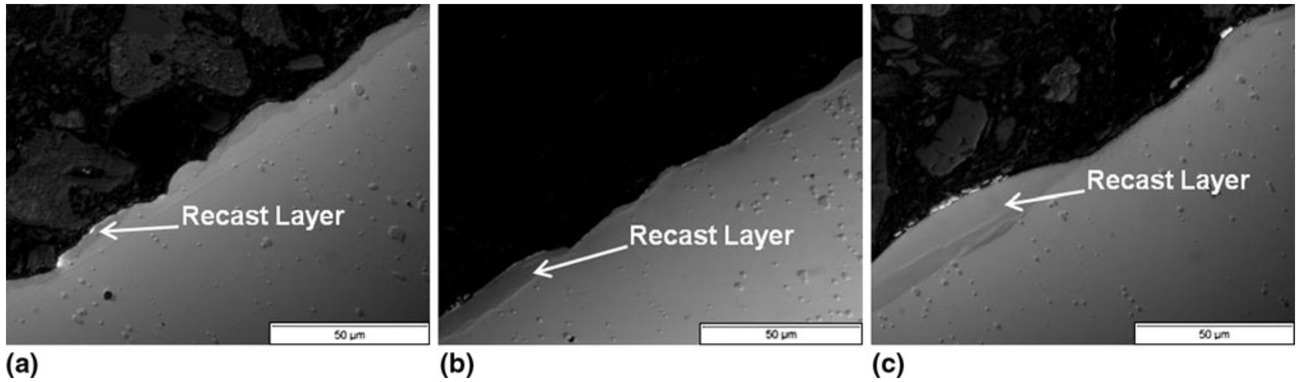

Fig. 12 EDM recast layers and roughness produced on gage surfaces of fatigue specimens with varied EDM processing conditions: (a) low, (b) standard, and (c) high

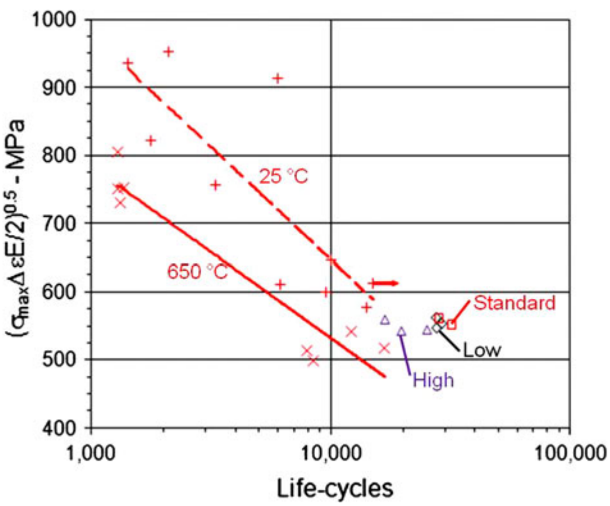

Fig. 13 Comparison of fatigue lives in hydrogen for all specimens tested at 25 and 650 °C, with those tested at 325 °C having low, standard, and high EDM surface conditions

may also not harm fatigue life. This could produce significant cost savings over other machining processes, especially for superalloys, which are known to be hard to machine. Screening of specimens prepared with varying EDM conditions, using fatigue tests at conditions relevant to an application, would be necessary to confirm and calibrate this response for other materials and applications of interest.

Additional tests would be necessary to estimate design-minimum fatigue lives under the present conditions. This could include replicate tests at current conditions, and additional tests at intermediate temperatures, strains, and strain ratios. Tests could also be targeted to simulate the conditions predicted for critical locations of a component, for further confidence in lives there.

4. Summary and Conclusions

In summary, low cycle fatigue capability of Haynes 188 was assessed at 25 and 650 °C in helium and hydrogen environ-

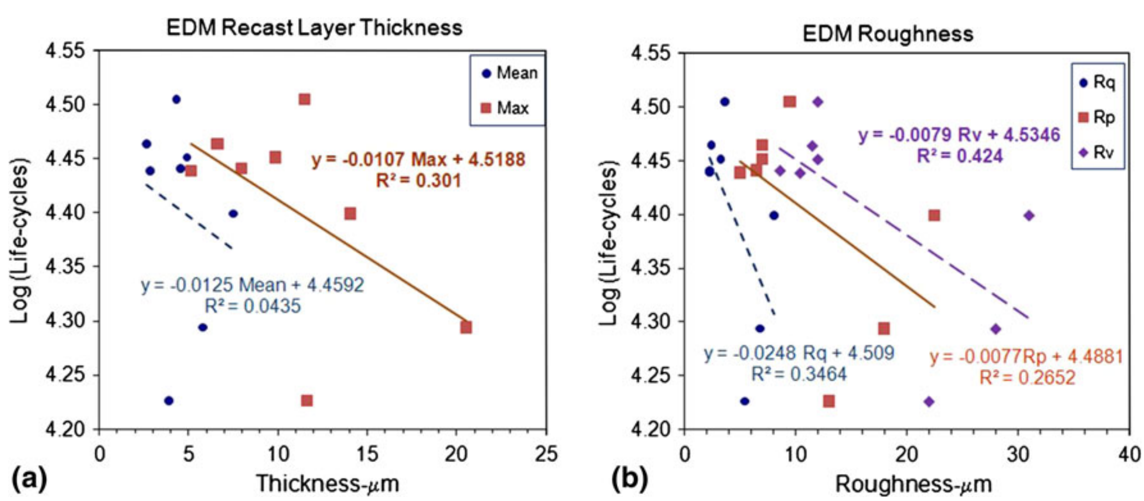

Fig. 14 Effects of surface conditions on fatigue lives of EDM specimens tested at 325 °C: (a) recast layer thickness and (b) roughness

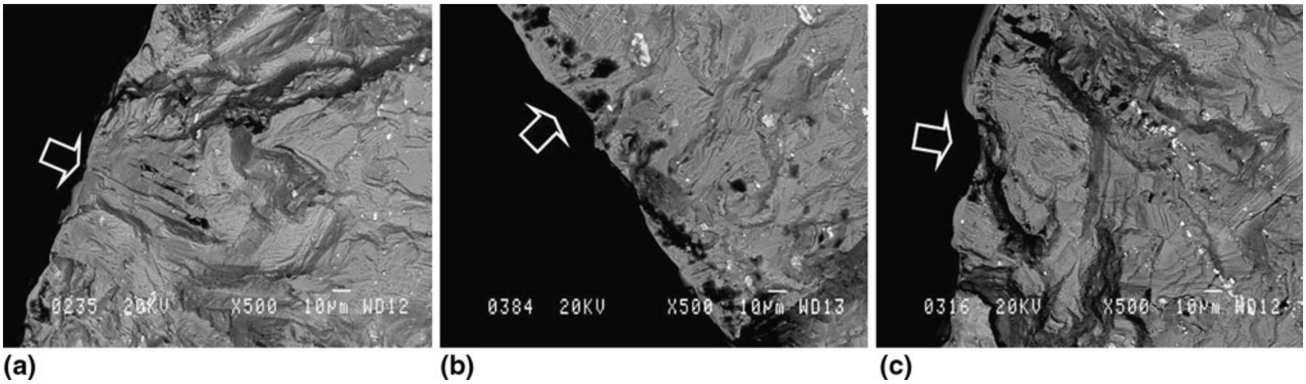

Fig. 15 Typical fatigue failure initiation sites for specimens tested at 325 °C in hydrogen having EDM conditions of: (a) low, (b) standard, and (c) high

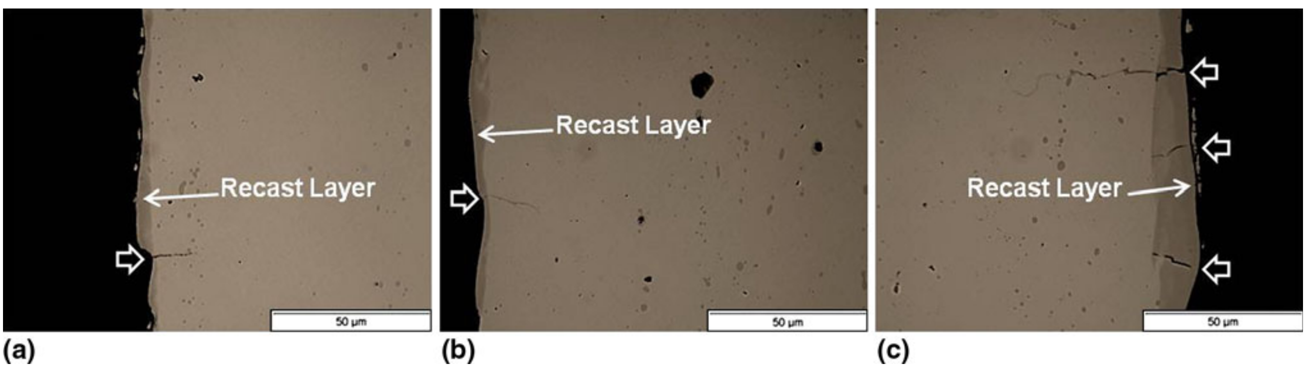

Fig. 16 Typical fatigue failure initiation sites for specimens tested at 325 °C in hydrogen having EDM conditions of: (a) low, (b) standard, and (c) high

ments. Specimens with LSG and electro-discharge machined specimen finishes were tested. Fatigue life decreased with increasing strain range, strain ratio, temperature, and with hydrogen atmosphere. A Smith-Watson-Topper stress parameter could be used to account for variations in strain range and strain ratio, and most strongly influenced life. Temperature and then atmosphere had decreasing effects on life. Reduced lives were observed for the combinations of hydrogen environment with low temperature, and high temperature with high stress. EDM finish did not consistently reduce mean fatigue life from that of LSG finish specimens. However, purposeful variation of EDM conditions to vary associated roughness and recast layer thickness around the standard conditions indicated "high" EDM settings could produce sufficiently high roughness and recast layer thickness to significantly decrease life.

It can be concluded that the low cycle fatigue life capability of Haynes 188 in high pressure hydrogen could be quite satisfactory, for applications such as hypersonic turbine engine components. While fatigue life decreased with increasing strain and temperature conditions, hydrogen effects were reduced with increasing temperature. Mean life capability was sustained even with a "standard" EDM surface preparation, potentially useful for cooling passages. This could be related to the superior ductility of this material.

Acknowledgments

The authors wish to acknowledge the support of the NASA Hypersonics Program, Anthony Calomino and Diego Capriotti. Also acknowledged are Tina Malone, Brian Hastings, Michael Watwood, and Eric King, manager and engineers at NASA Marshall Space Flight Center overseeing the Hydrogen Fatigue Testing facility and fatigue testing machines.

References

1. R.R. Kazmar, Airbreathing Hypersonic Propulsion at Pratt & Whitney-Overview, *13th AIAA/CIRA International Space Planes Symposium*, AIAA, 2005
2. A.H. Auslender, K.L. Suder, and S.R. Thomas, An Overview of the NASA FAP Hypersonics Project Airbreathing Propulsion Research, *AIAA Proceedings*, [np]. 19–22 Oct 2009
3. Haynes 188 Alloy, Technical Publication H-3001B, Haynes International, Inc., 2000
4. J.A. Harris and M.C. Van Wanderham, *Properties of Materials in High Pressure Hydrogen at Cryogenic, Room, and Elevated Temperatures*, NASA CR NAS8-26191, Washington, D.C., 1973
5. K.N. Smith, P. Watson, and T.H. Topper, A Stress-Strain Function for the Fatigue of Metals, *J. Mater.*, 1970, **5**, p 767–778
6. S. Kalluri, M.A. McGaw, and G.R. Halford, *Fatigue Life Estimation Under Cumulative Cyclic Loading Conditions*, ASTM STP 1389, ASTM, West Conshohocken, PA, 2000, p 94–109

7. J. Sall, L. Creighton, and A. Lehman, *JMP Start Statistics: A Guide to Statistics and Data Analysis Using JMP and JMP IN Software*, SAS Institute Inc., Cary, NC, 2005
8. R.J. Walter and J.D. Frandsen, Fractography of Alloys Tested in High-Pressure Hydrogen, *Proc. of the Symposium Hydrogen Effects in Metals*, TMS, 1981, p 819–827